

---

# A Basic Evaluation of Neural Networks Trained with the Error Diffusion Learning Algorithm

---

**Kazuhiisa Fujita**

Komatsu University, 10-10 Doihara-Machi, Komatsu, Ishikawa, Japan 923-0921  
kazu@spikingneuron.net

## Abstract

Artificial neural networks are powerful tools capable of addressing various tasks. Although the backpropagation algorithm has become a standard training method for these neural networks, its lack of biological plausibility has inspired the development of alternative learning approaches. One such alternative is Kaneko's Error Diffusion Learning Algorithm (EDLA), a biologically motivated approach wherein a single global error signal diffuses throughout a network composed of paired excitatory-inhibitory sublayers, thereby eliminating the necessity for layer-wise backpropagation. This study presents a contemporary formulation of the EDLA framework and evaluates its effectiveness through parity check, regression, and image classification tasks. Our experimental results indicate that EDLA networks can consistently achieve high accuracy across these benchmarks, with performance efficiency and convergence speed notably influenced by the choice of learning rate, neuron count, and network depth. Further investigation of the internal representations formed by EDLA networks reveals their capacity for meaningful feature extraction, similar to traditional neural networks. These results suggest that EDLA is a biologically motivated alternative for training feedforward networks and will motivate future work on extending this method to biologically inspired neural networks.

## 1 Introduction

Artificial neural networks have substantially advanced numerous research domains, including image processing, signal processing, and natural language processing. The remarkable success of these networks largely stems from the backpropagation method proposed by Rumelhart et al. (1986), which has become a standard method for training neural networks across diverse architectures.

The theoretical foundation of neural networks can be traced back to the linear neuron threshold model introduced by McCulloch and Pitts (1943); McCulloch and Pitts (1943). The fundamental mechanism of this model is based on the all-or-none law (Adrian (1914); Kato (1926)) and still underlies modern neural network architectures. Rosenblatt's development of the perceptron (Rosenblatt (1958)) represents another critical milestone in neural networks, marking the first realization of a trainable artificial neuron. However, a single-layer structure of perceptrons does not inherently have the capability to create nonlinear decision boundaries. Although multilayer perceptrons (MLPs) resolve this limitation, training these deeper networks has been a substantial challenge. The introduction of backpropagation provided a solution for training MLPs, and subsequently became the dominant paradigm for training various deep neural network architectures.

Despite the success of backpropagation, its biological plausibility has been questioned (Crick:1989, Mostafa:2018). This gap between artificial and biological neural systems has motivated the development of alternative learning algorithms. One example is Kaneko's Error Diffusion Learning Algorithm (EDLA)

citeKaneko. EDLA introduces a biologically inspired architecture that incorporates both excitatory and inhibitory synapses, reflecting biological neural systems more closely. The distinctive feature of this algorithm is its error-diffusion mechanism. In this approach, the difference between the network output and target values is diffused throughout the network during training, resulting in efficient training of sigmoid neural networks. Unlike standard backpropagation, the EDLA diffuses only a single error signal throughout the network, eliminating the need for backward propagation and error calculation for each layer. This simplification addresses one of the key problems highlighted by Mostafa (2018), which artificial neural networks based on backpropagation require buffering past presynaptic activities and synchronizing them with the corresponding error signals propagated sequentially from higher layers.

This study provides a comprehensive overview of the EDLA framework and evaluates its performance on several benchmark tasks including parity checks, image classification, and regression. Through these evaluations, we aim to promote the EDLA framework and facilitate the development of training methods for biologically plausible neural networks.

## 2 Multi-Layer Perceptron and Backpropagation

A multilayer perceptron (MLP) is a class of feedforward artificial neural networks characterized by multiple interconnected neuron layers: an input layer, one or more hidden layers, and an output layer. Typically, each neuron within one layer is fully connected to all neurons in the subsequent layer.

The input to an MLP is represented by the vector  $\mathbf{x} = [x_0, x_1, \dots, x_N]^T \in \mathbb{R}^{N+1}$ , where  $x_0$  commonly serves as a bias term (usually set as  $x_0 = 1$ ) and  $N$  denotes the number of input features. This input vector is received by the input layer and subsequently propagated forward to the first hidden layer.

For neuron  $j$  in the first hidden layer ( $l = 1$ ), the activation  $a_j^{(1)}$  is calculated as the weighted sum of its inputs:

$$a_j^{(1)} = \mathbf{w}_j^{(1)T} \mathbf{x} \quad (1)$$

where  $\mathbf{w}_j^{(1)} = [w_{j0}^{(1)}, w_{j1}^{(1)}, \dots, w_{jN}^{(1)}]^T$  represents the weight vector connecting the input layer to neuron  $j$  in the first hidden layer ( $l$ ). Here,  $w_{ji}^{(1)}$  denotes the weight connecting from the neuron  $i$  in the input layer to the neuron  $j$  in the first hidden layer. The output of neuron  $j$  is then obtained by applying the activation function  $g(\cdot)$ :

$$z_j^{(1)} = g(a_j^{(1)}). \quad (2)$$

For subsequent hidden layers ( $l = 2, \dots, L$ ), the activation  $a_j^{(l)}$  for neuron  $j$  in layer  $l$  is computed as follows:

$$a_j^{(l)} = \mathbf{w}_j^{(l)T} \mathbf{z}^{(l-1)}, \quad (3)$$

where  $\mathbf{z}^{(l)} = [z_0^{(l)}, z_1^{(l)}, \dots, z_{M^{(l)}}^{(l)}]^T \in \mathbb{R}^{M^{(l)}+1}$  is the output vector of layer  $l$ ,  $M^{(l)}$  is the number of neurons in this layer, and  $z_0^{(l)}$  corresponds to the output of a bias neuron fixed at one.  $w_{ji}^{(l)}$  denotes the weight connecting neuron  $i$  in layer  $l-1$  to neuron  $j$  in layer ( $l$ ). The output for neuron  $j$  is then given by

$$z_j^{(l)} = g(a_j^{(l)}). \quad (4)$$

Finally, the output for neuron  $k$  in the output layer ( $L+1$ ) is similarly computed as:

$$y_k = f(a_k^{(L+1)}) = f(\mathbf{w}_k^{(L+1)T} \mathbf{z}^{(L)}) \quad (5)$$

where  $f(\cdot)$  is the activation function for the output neurons, and  $\mathbf{w}_k^{(L+1)}$  is the weight connecting the neurons in the final hidden layer ( $L$ ) to output neuron  $k$ .

Training an MLP seeks the optimal weights  $\mathbf{w}$  that minimize a predetermined loss function  $E(\mathbf{w})$ , such as mean squared error or cross-entropy loss. Gradient descent is a widely used optimization method, in which weights are iteratively updated in the direction that locally reduces the value of  $E(\mathbf{w})$ . To efficiently compute gradients necessary for this optimization, the backpropagation algorithm employs the chain rule, propagating the error signals sequentially from the output layer backward through each hidden layer to the input layer.

Consider an output neuron  $k$  in the output layer ( $L + 1$ ). Using the chain rule, the partial derivative of the loss function  $E(\mathbf{w})$  with respect to the weight  $w_{kj}^{(L+1)}$  connecting neuron  $j$  in the last hidden layer ( $L$ ) to neuron  $k$  in the output layer is computed as follows:

$$\frac{\partial E(\mathbf{w})}{\partial w_{kj}^{(L+1)}} = \frac{\partial E(\mathbf{w})}{\partial a_k^{(L+1)}} \frac{\partial a_k^{(L+1)}}{\partial w_{kj}^{(L+1)}} = \delta_k^{(L+1)} z_j^{(L)} \quad (6)$$

where

$$\delta_k^{(L+1)} \equiv \frac{\partial E(\mathbf{w})}{\partial a_k^{(L+1)}} = f'(a_k^{(L+1)}) \frac{\partial E(\mathbf{w})}{\partial y_k}. \quad (7)$$

This quantity, often referred to as the error for output neuron  $k$ , is the partial derivative of the loss  $E(\mathbf{w})$  with respect to the neuron's activation  $a_k^{(L+1)}$ . By chain rule, this derivative can be factored into two components: the partial derivative of the loss function with respect to the neuron's output,  $\frac{\partial E(\mathbf{w})}{\partial y_k}$ , and the derivative of the activation function evaluated at  $a_k^{(L+1)}$ , namely  $f'(a_k^{(L+1)})$ .

To calculate the error  $\delta_j^{(l)}$  for hidden layer ( $l$ ), we make use of the chain rule again. The partial derivative of the error function with respect to the activation  $a_j^{(l)}$  is:

$$\frac{\partial E(\mathbf{w})}{\partial w_{ji}^{(l)}} = \frac{\partial E(\mathbf{w})}{\partial a_j^{(l)}} \frac{\partial a_j^{(l)}}{\partial w_{ji}^{(l)}} = \delta_j^{(l)} z_i^{(l-1)}. \quad (8)$$

The error  $\delta_j^{(l)}$  is defined as:

$$\delta_j^{(l)} \equiv \frac{\partial E(\mathbf{w})}{\partial a_j^{(l)}} = g'(a_j^{(l)}) \sum_k \delta_k^{(l+1)} w_{kj}^{(l+1)}, \quad (9)$$

where  $g'(\cdot)$  represents the derivative of the activation function  $g(\cdot)$  evaluated at  $a_j^{(l)}$ . Intuitively, the error at hidden neuron  $j$  is computed based on the weighted sum of error signals from the neurons in the subsequent layer ( $l + 1$ ), thus sequentially propagating the error signal backward through the network.

Once the partial derivatives  $\frac{\partial E(\mathbf{w})}{\partial w_{ji}^{(l)}}$  are computed for all weights, the update rule in standard gradient descent is:

$$w_{ji}^{(l)} \leftarrow w_{ji}^{(l)} - \eta \frac{\partial E(\mathbf{w})}{\partial w_{ji}^{(l)}}, \quad (10)$$

where  $\eta$  is the learning rate. This iterative cycle—consisting of a forward pass (computation of neuron activations), a backward pass (error computation), and weight updates—continues until a predetermined convergence criterion is satisfied or a specified number of training epochs has been reached.

The gradient of the error function with respect to the weights is computed using training data. In practice, to compute the gradient, most practitioners use a method called stochastic gradient descent (SGD) LeCun et al. (2015). In SGD, the calculation of the gradient is performed on a subset of the training data, known as a mini-batch. This approach enables efficient computation of the gradient, making it feasible to train large neural networks using extensive datasets.

### 3 Error Diffusion Learning Algorithm (EDLA)

The Error Diffusion Learning Algorithm (EDLA) is a novel approach to neural network learning initially proposed by Kaneko Kaneko (2008). Although the original model is available only in Japanese, this section provides a comprehensive reinterpretation of EDLA.

#### 3.1 Network Architecture

Figure 1 illustrates the neural network architecture employed by the EDLA. Similar to traditional MLPs, EDLA adopts a multilayer structure comprising neurons and synapses. However, EDLA

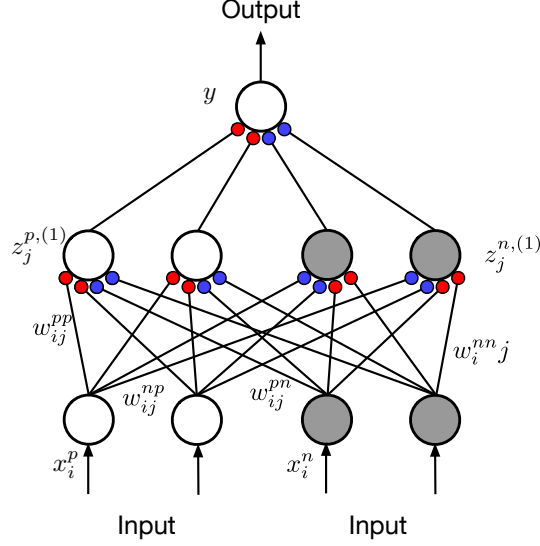


Figure 1: Schematic representation of the Error Diffusion Learning Algorithm (EDLA) network architecture. The network consists of multiple layers of positive neurons (white circles) and negative neurons (gray circles). The red and blue small circles at the connections indicate excitatory and inhibitory synapses, respectively.

incorporates two types of neurons: positive neurons (p-neurons) and negative neurons (n-neurons). The synaptic connections are categorized based on the types of neurons they link: excitatory synapses connect neurons of identical type, whereas inhibitory synapses connect neurons of different types. A key characteristic of the EDLA is that it has only one output neuron.

### 3.2 Learning Rule and Mathematical Formulation

The input to the EDLA network is represented by the vector  $\mathbf{x} = [x_0, x_1, \dots, x_N]^T \in \mathbb{R}^{N+1}$ , where  $x_0$  corresponds to the output of the bias neuron set to one. In the EDLA architecture, each layer consists of positive and negative sublayers. Consequently, the outputs from the positive and negative sublayers of the input layer are denoted by  $\mathbf{x}^p$  and  $\mathbf{x}^n$ , respectively. For the input layer  $\mathbf{x}^p = \mathbf{x}^n = \mathbf{x}$ . For a neuron  $j$  in the first hidden layer ( $l = 1$ ), the activations for the positive and negative neurons,  $a_j^{p,(1)}$  and  $a_j^{n,(1)}$ , are computed as follows:

$$a_j^{p,(1)} = \mathbf{w}_j^{pp,(1)T} \mathbf{x}^p + \mathbf{w}_j^{pn,(1)T} \mathbf{x}^n, \quad (11)$$

$$a_j^{n,(1)} = \mathbf{w}_j^{np,(1)T} \mathbf{x}^p + \mathbf{w}_j^{nn,(1)T} \mathbf{x}^n. \quad (12)$$

In these equations,  $\mathbf{w}_j^{pp,(1)} = [w_{j1}^{pp}, \dots, w_{jN}^{pp}]^T$  represents the vector of synaptic weights connecting the positive neurons in the input layer to the positive neuron  $j$  in the first hidden layer ( $l = 1$ ). Similarly,  $\mathbf{w}_j^{pn,(1)}$ ,  $\mathbf{w}_j^{np,(1)}$ , and  $\mathbf{w}_j^{nn,(1)}$  denote the weight vectors for the other combinations of neuron types in the connections between the input and first hidden layers.

The outputs of the positive and negative neurons  $j$  in the first hidden layer are given by:

$$z_j^{p,(1)} = g(a_j^{p,(1)}) \quad \text{and} \quad z_j^{n,(1)} = g(a_j^{n,(1)}) \quad (13)$$

where  $g(\cdot)$  is the activation function. In subsequent hidden layers ( $l = 2, \dots, L$ ) where  $L$  refers to the final hidden layer, the neuron outputs are given by

$$z_j^{p,(l)} = g(\mathbf{w}_j^{pp,(l)T} \mathbf{z}^{p,(l-1)} + \mathbf{w}_j^{pn,(l)T} \mathbf{z}^{n,(l-1)}), \quad (14)$$

$$z_j^{n,(l)} = g(\mathbf{w}_j^{np,(l)T} \mathbf{z}^{p,(l-1)} + \mathbf{w}_j^{nn,(l)T} \mathbf{z}^{n,(l-1)}). \quad (15)$$

The final output of the EDLA network  $y$  is computed as

$$y = g(\mathbf{w}^{pp,(L+1)T} \mathbf{z}^{p,(L)} + \mathbf{w}^{pn,(L+1)T} \mathbf{z}^{n,(L)}). \quad (16)$$

Synaptic weights within the EDLA network are constrained to maintain specific relationships, reflecting the excitatory and inhibitory nature of the connections:

$$w_{ji}^{pp,(l)} \geq 0, \quad w_{ji}^{pn,(l)} \leq 0, \quad w_{ji}^{np,(l)} \leq 0, \quad w_{ji}^{nn,(l)} \geq 0. \quad (17)$$

The objective of training an EDLA network is to identify the optimal parameter set  $\mathbf{w}$  that minimizes a predefined error function  $E(\mathbf{w})$ , similar to traditional standard MLPs. Although EDLA utilizes the principles of the gradient descent method, it incorporates an approximation to compute the errors (partial derivatives of the loss function). Specifically, the approximated errors,  $\tilde{\delta}_{ji}^{pp}$ ,  $\tilde{\delta}_{ji}^{np}$ ,  $\tilde{\delta}_{ji}^{nn}$ , and  $\tilde{\delta}_{ji}^{pn}$  in EDLA are expressed as:

$$\tilde{\delta}_{ji}^{pp,(l)} = dg'(a_j^{p,(l)}), \quad \tilde{\delta}_{ji}^{np,(l)} = dg'(a_j^{n,(l)}), \quad (18)$$

$$\tilde{\delta}_{ji}^{nn,(l)} = dg'(a_j^{n,(l)}), \quad \tilde{\delta}_{ji}^{pn,(l)} = dg'(a_j^{p,(l)}), \quad (19)$$

where global error  $d$  is defined as  $d = -\frac{\partial E(\mathbf{w})}{\partial y}$ . For example,  $d > 0$  indicates that the network output is smaller than the target value and must increase when the L2 norm is used as the error function (see the next subsection for details). A key deviation from the standard gradient descent method lies in EDLA's approximation of the error computation, which utilizes the error  $\frac{\partial E(\mathbf{w})}{\partial y}$  from the output layer instead of directly propagating errors  $\delta$ s from subsequent layers. In an MLP, the errors  $\delta$  are computed for each neuron in the network and propagated backward through the network. In contrast, EDLA employs a single error signal  $d$  that is uniformly diffused throughout the entire network. This diffusion mechanism simplifies the learning process by eliminating the need for individual error calculations in each layer. This diffusion mechanism is a unique feature of EDLA that distinguishes it from traditional backpropagation methods.

The weight updates in EDLA differ depending on the sign of the global error  $d$ . When  $d > 0$ , indicating a positive error, the weights originating from the positive neurons  $w_{ji}^{pp,(l)}$  and  $w_{ji}^{np,(l)}$  are updated as follows:

$$w_{ji}^{pp,(l)} \leftarrow w_{ji}^{pp,(l)} + \eta \tilde{\delta}_{ji}^{pp,(l)} z_i^{p,(l-1)} = w_{ji}^{pp,(l)} + \eta dg'(a_j^{p,(l)}) z_i^{p,(l-1)}, \quad (20)$$

$$w_{ji}^{np,(l)} \leftarrow w_{ji}^{np,(l)} - \eta \tilde{\delta}_{ji}^{np,(l)} z_i^{p,(l-1)} = w_{ji}^{np,(l)} - \eta dg'(a_j^{n,(l)}) z_i^{p,(l-1)}. \quad (21)$$

Conversely, when  $d < 0$ , indicating a negative error, the weights originating from the negative neurons,  $w_{ji}^{nn,(l)}$  and  $w_{ji}^{pn,(l)}$  are updated as:

$$w_{ji}^{nn,(l)} \leftarrow w_{ji}^{nn,(l)} - \eta \tilde{\delta}_{ji}^{nn,(l)} z_i^{n,(l-1)} = w_{ji}^{nn,(l)} - \eta dg'(a_j^{n,(l)}) z_i^{n,(l-1)}, \quad (22)$$

$$w_{ji}^{pn,(l)} \leftarrow w_{ji}^{pn,(l)} + \eta \tilde{\delta}_{ji}^{pn,(l)} z_i^{n,(l-1)} = w_{ji}^{pn,(l)} + \eta dg'(a_j^{p,(l)}) z_i^{n,(l-1)}. \quad (23)$$

where  $\eta$  is the learning rate. Thus, the global error signal directly determines whether the positive or negative neuron weights are adjusted during the training.

For the EDLA, the activity function is typically selected as the sigmoid function  $g(a) = 1/(1 + \exp(-a))$ , which ensures that the neuron outputs remain within the interval  $[0, 1]$ . Each weight update is computed proportionally to the product of a single global error signal and the output of the corresponding neuron. By constraining the neuron outputs to this limited range, the sigmoid activation function provides stability to the training dynamics, effectively reducing excessively large weight adjustments and facilitating stable convergence.

### 3.3 Biological Interpretation

The behavior of the Error Diffusion Learning Algorithm (EDLA) becomes intuitively clear when employing the sigmoid activation function along with the squared-error loss function defined as  $E(\mathbf{w}) = \frac{1}{2}(y - t)^2$ . Under this formulation, the global error signal  $d$  is represented as follows:

$$d = -\frac{\partial E(\mathbf{w})}{\partial y} = -\frac{\partial}{\partial y} \left[ \frac{1}{2}(y - t)^2 \right] = t - y. \quad (24)$$

When the network output is smaller than the target value ( $d > 0$ ), the absolute values of the weights originating from positive neurons increase due to the properties  $g'(a) > 0$  and  $z > 0$ . Such weight adjustments amplify the outputs of positive neurons in subsequent layers while simultaneously suppressing the outputs of negative neurons in those layers. Conversely, when the network output exceeds the target value ( $d < 0$ ), the absolute values of the weights originating from the negative neurons increase. These weight adjustments decrease the outputs of positive neurons in subsequent layers while simultaneously increasing the outputs of negative neurons. Thus, regardless of the sign of the global error signal, EDLA systematically reduces the difference between the network output and target values through successive weight updates. Importantly, this characteristic learning behavior of EDLA is maintained as long as  $g'(a) > 0$ ,  $z > 0$ , and the sign of the derivative of the loss function properly encodes whether the network output is below or above the target value.

In the EDLA framework, the global error signal  $d$  functions as a plasticity-guiding neuromodulatory signal, orchestrating synaptic weight updates through the coordinated activities of the presynaptic and postsynaptic neurons. This concept is strongly reminiscent of Hebbian learning Hebb (1949), which posits that changes in the synaptic strength are driven by correlated neuronal activation patterns. Specifically, the EDLA learning rule, represented by  $\eta d g'(a_j^{p,(l)}) z_i^{p,(l-1)}$  for the synaptic weights  $w_{ji}^{pp,(l)}$ , is proportional to the product of the derivative of the postsynaptic neuron’s activation function  $g'(a_j^{p,(l)})$  and the output of the presynaptic neuron  $z_i^{p,(l-1)}$ . This mathematical relationship can be interpreted as a Hebbian-like plasticity mechanism, wherein weight adjustments reflect a direct interaction between the activities of presynaptic (characterized by  $z_i^{p,(l-1)}$ ) and postsynaptic neurons (captured by  $g'(a_j^{p,(l)})$ ).

Moreover, EDLA employs a global error signal diffusion mechanism, in which the error signal  $d$  uniformly propagates throughout the entire network. This diffusion process is conceptually analogous to biological neuromodulation and closely parallels the reward prediction error (RPE) mechanism observed in biological neural systems, which guides synaptic plasticity across neural circuits via diffuse neuromodulatory signals Roelfsema and Holtmaat (2018). This neuromodulatory-inspired global diffusion effectively orchestrates all synaptic modifications in the network; thereby, this mirrors biological processes wherein neuromodulators such as dopamine broadly regulate neural plasticity based on RPE signals.

### 3.4 Limitation

The inherent simplicity and approximation underlying EDLA introduce significant constraints, particularly concerning the network’s capability to effectively handle multiple outputs. In the EDLA framework, the global error signal  $d$  is uniformly diffused throughout the network architecture. This global error diffusion inherently directs the optimization process toward minimizing the error associated with a single output node. Consequently, when dealing with single-output scenarios, EDLA can efficiently and accurately specialize the network weights for that specific output. However, when an EDLA network contains multiple outputs, each output generates its own global error signal that propagates throughout the network. Such simultaneous diffusion of distinct error signals leads to conflicting weight adjustments as the network simultaneously attempts to minimize errors for multiple outputs. These conflicting updates inhibit the network’s ability to extract and generalize meaningful features from the input data, undermining the learning efficacy.

In contrast, traditional MLPs have an advantage when handling network architectures requiring multiple outputs. MLPs can simultaneously optimize the weights associated with each output. This is attributed to the backpropagation mechanism in MLPs, where the weights connecting the output layer to the preceding hidden layer are specifically adjusted to minimize the error associated with each output. Concurrently, hidden-layer neurons are trained to extract and generalize pertinent features from the input data. This hierarchical optimization enables MLPs to efficiently model complex input-output relationships and successfully generalize the learned features. Consequently, MLPs with backpropagation provide a more flexible learning mechanism than EDLA.

### 3.5 Extending EDLA to Multiple Outputs

The inherent single-output constraint of the EDLA represents a significant limitation when addressing tasks that require multiple outputs. A simple approach to adapting EDLA to overcome this limitation involves constructing multiple EDLA networks arranged in parallel. This parallelized architecture addresses a task requiring  $K$  outputs by employing  $K$ -independent EDLA networks. Each individual network retains the fundamental EDLA architecture and operates autonomously. Input vector  $\mathbf{x}$  is simultaneously provided to all networks, ensuring that they process the same input data. Each network independently computes output  $y_k$ , where  $k \in \{1, \dots, K\}$ . In classification tasks, if the output  $y_k$  is the maximum value among the outputs of the EDLA networks,  $k$  is regarded as the overall output label.

The weights of each individual EDLA network are independently optimized using the standard EDLA update rule. Consequently, this parallel architecture retains the capability, simplicity, and core principles inherent to single-output EDLA models, effectively extending EDLA’s capability to handle multioutput tasks. However, this parallelization approach increases the computational costs because the total number of EDLA networks scales linearly with the required number of outputs. This trade-off shows the challenge of maintaining the computational simplicity of single-output EDLA networks while contending with the additional resource demands necessary for multioutput learning.

Employing multiple single-output networks in an EDLA framework may initially seem computationally inefficient compared with traditional multi-output MLP architectures. Nevertheless, this modular approach closely resembles the organizational principles observed in biological neural systems, particularly in the brain Casanova and Casanova (2018). Mountcastle’s early neurophysiological research Mountcastle (1957) demonstrated that neurons within the primate somatosensory cortex are organized into vertically aligned columns, with each column dedicated to a particular modality or receptive field. Additionally, neurons in the primary visual cortex are organized into modular structures known as hypercolumns, each specializing in processing specific features of visual stimuli such as orientation Hubel and Wiesel (1968). Each hypercolumn functions semi-independently, collectively contributing to overall visual perception by handling distinct components of the visual scene. Similarly, the inferior temporal (IT) cortex exhibits clusters of neurons that are selectively responsive to complex visual features including distinct object shapes Sato et al. (2008); Tanaka (1996). This clustered arrangement enables the efficient processing of diverse visual elements while simultaneously facilitating effective integration across features and categories. Another notable example is the barrel cortex of rodents, in which neural clusters (called barrels) are dedicated to independently processing tactile inputs from individual whiskers Li and Crair (2011); Woolsey and Van der Loos (1970). Each barrel independently processes sensory information corresponding to its associated whisker, and the combined neural activity across the barrels generates a comprehensive tactile representation. These modular and distributed neural processing strategies enable the brain to handle complex and heterogeneous tasks efficiently while preserving both flexibility and robustness. Although the parallelized architecture of EDLA, which consists of multiple single-output networks dedicated to specific outputs, may be computationally less efficient than traditional multi-output MLPs, it reflects these biological modular architectures.

## 4 Experimental Setup

The neural networks are implemented in Python, using NumPy for linear algebra operations and PyTorch for neural networks. The source code is available on GitHub at <https://github.com/KazuhisaFujita/EDLA> for reproducibility and further extension of this work.

## 5 Experimental Results

### 5.1 Parity Check Task

To evaluate the efficacy of the Error Diffusion Learning Algorithm (EDLA), we initially assessed its performance on a parity check task, a classical benchmark in neural network learning. This task involves determining whether the number of ones in a binary input vector is even or odd. The parity check task is a two-class classification problem. The EDLA network consists of an input layer, hidden layers, and an output layer. The neurons in the input and the hidden layers use the sigmoid or ReLU

activation functions. The output neuron is singular and employs the sigmoid activation function, producing a value between 0 and 1. The output is interpreted as the probability of the input vector containing an odd number of ones. Thus, the output neuron is expected to yield a value above 0.5 for odd counts and below 0.5 for even counts. The total number of possible input combinations is  $2^{n_{\text{bit}}}$ , where  $n_{\text{bit}}$  denotes the number of bits in the input vector. In this experiment,  $n_{\text{bit}} = 2, 3, 4, 5$  with each dataset including all possible combinations for a given  $n_{\text{bit}}$ . A mini-batch size of 4 is consistently employed across all configurations.

Figure 2 illustrates the performance of the EDLA network with a single hidden layer and sigmoid activation function across various learning rates (0.1, 1.0, 10.0) and neuron counts per layer (8, 16, 32, 64, 128). The results demonstrate that the EDLA network achieves high accuracy on the parity check task. Notably, except for configurations with eight neurons when  $n_{\text{bit}} = 5$ , the network attains perfect accuracy across all cases. The number of epochs required to reach an accuracy of 0.9 decreases as the number of neurons increases. For the learning rates of 10 and 1.0, the convergence time (reach epoch) is smaller than the learning rate of 0.1. Furthermore, for  $n_{\text{bit}} \in \{3, 5\}$ , the reach epoch at a learning rate of 1.0 is nearly identical to that at a learning rate of 10. For  $n_{\text{bit}} = 2$ , the reach-epoch for a learning rate of 1.0 is larger than that at a learning rate of 10, but for  $n_{\text{bit}} = 4$  the reach epoch at a learning rate of 1.0 is smaller than that at a learning rate of 10. These results suggest that learning rates of 10 and 1.0 enable efficient training.

Figure 3 presents an analysis of the performance of the EDLA network using the sigmoid activation function across various hidden layers (1, 2, 4, and 8 hidden layers) and neuron counts per layer with a fixed learning rate of 1.0. The results reveal that the accuracy consistently approaches or reaches 1.0 across different bit numbers ( $n_{\text{bit}}$ ), regardless of the number of hidden layers ranging from one to eight. However, the number of epochs required to achieve 0.9 accuracy reveals more nuanced dependencies on the network depth and neuron count. Specifically, for  $n_{\text{bit}} = 2$ , shallow networks (one layer) exhibit a relatively low reach epoch for smaller neuron numbers, but the reach epoch increased for larger neuron counts. The deeper networks do not exhibit significant reach epoch reductions for  $n_{\text{bit}} = 2$ . Conversely, for  $n_{\text{bit}} \in \{3, 4\}$  with deeper architectures (four and eight layers), the reach epoch increases with the number of neurons. For  $n_{\text{bit}} = 5$ , the reach epoch decreases notably with the neuron count and stabilized for neuron counts of 64 and above. These results indicate that EDLA networks with sigmoid activation can consistently achieve high accuracy on the parity check task, with optimal performance depending on the complexity of the task and the chosen network configuration.

Figure 4 shows the performance of the EDLA network with a single hidden layer and the ReLU activation function across various learning rates (0.01, 0.1, 1.0) and neuron counts of the hidden layer. For learning rates of 0.01 and 0.1, the network achieves high accuracy on the parity check task, with the number of epochs required to reach an accuracy of 0.9, decreasing as the number of neurons increases. The learning rate of 0.01 exhibits a slower convergence speed than a learning rate of 0.1, particularly for smaller neuron counts. For a learning rate of 1.0, the performance is worse than that for the other learning rates. In particular, for  $n_{\text{bit}} \in \{4, 5\}$ , the network fails to achieve an accuracy of 0.9 even with a large number of neurons. This shows that a learning rate of 1.0, which is too high for the EDLA network with the ReLU activation function, leads to instability in training and poor performance.

Figure 5 shows the accuracy and convergence speed of the EDLA network with ReLU activation across various neuron counts and hidden layer depths. Both the accuracy and convergence speed improve with increasing neuron count in the ReLU network. However, this improvement in convergence speed does not continue indefinitely and eventually plateaued. These results indicate a performance comparable to sigmoid-based networks, with a consistently faster convergence observed for ReLU-based configurations. This enhanced convergence speed arises from the absence of an upper bound in the ReLU activation function, facilitating larger weight updates.

## 5.2 Regression Tasks

The EDLA network is evaluated on regression tasks using three benchmark datasets: Airfoil Self-Noise, Concrete Compressive Strength, and Energy Efficiency. The Airfoil Self-Noise dataset comprises 1503 samples with five features and a target variable representing the sound pressure level. The Concrete Compressive Strength dataset includes 1030 samples with eight features and a target variable denoting the compressive strength of concrete. The Energy Efficiency dataset comprises 768

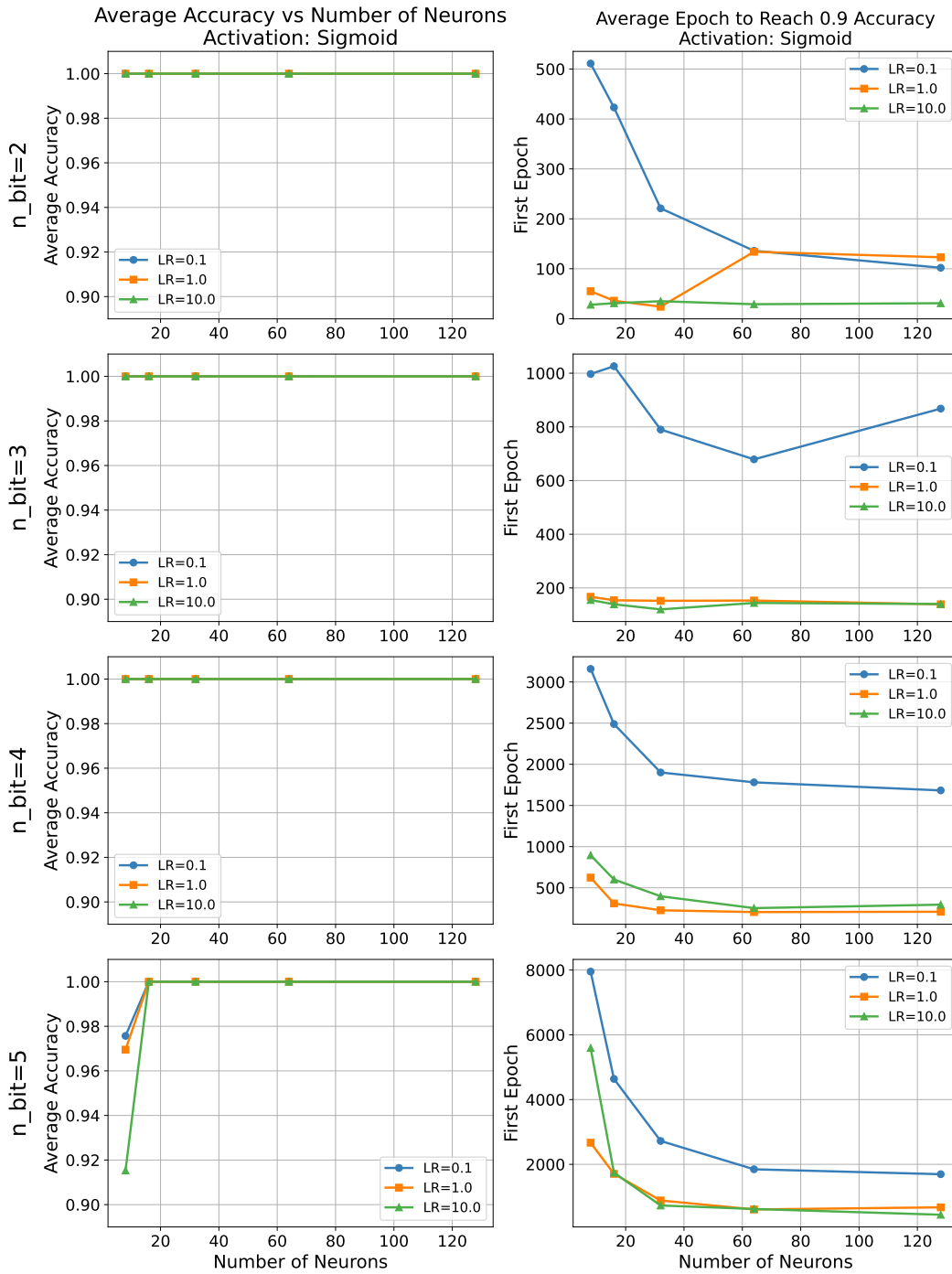


Figure 2: Performance of EDLA with sigmoid activation across various learning rates on the parity check task. The left column depicts the accuracy of the EDLA network with the sigmoid activation function as a function of neurons in a single hidden layer for different learning rates (LR = 0.1, 1.0, 10.0). The accuracies are averaged from 19900 to 20000 epochs. The right column shows the number of epochs required to reach an accuracy of 0.9 as a function of neurons in a hidden layer for the same learning rates. Each row of plots corresponds to a different bit length ( $n_{bit}$ , ranging from 2 to 5), for the parity check task. The results are averaged over ten independent trials.

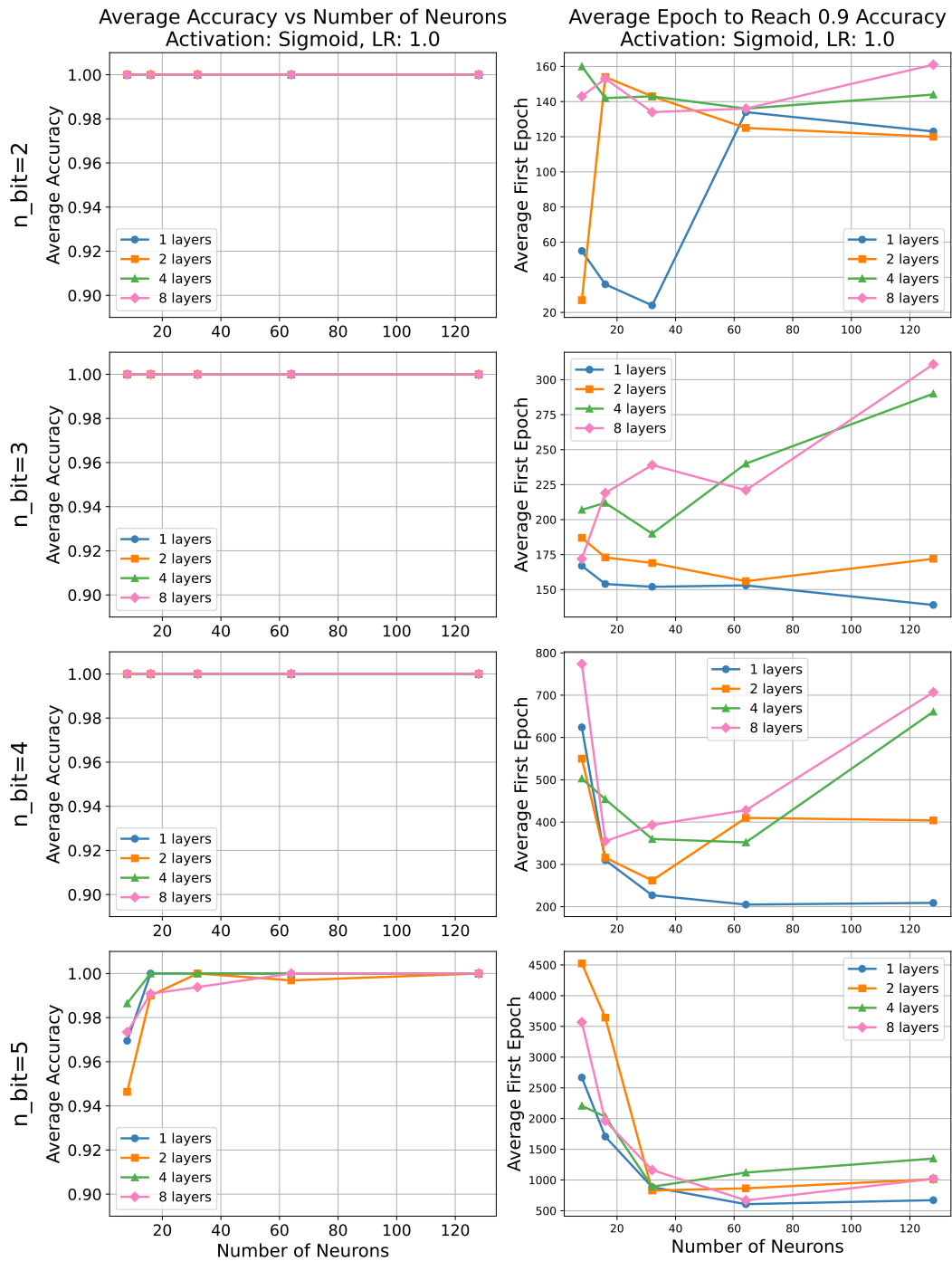


Figure 3: Accuracy and convergence characteristics of the EDLA network with sigmoid activation across various network depths (1, 2, 4, and 8 hidden layers) at a fixed learning rate of 1.0. The left column shows the average classification accuracy as a function of the neurons per hidden layer. The accuracies are average from 19900 to 20000 epochs. The right column presents the number of epochs required to reach an accuracy of 0.9 as a function of neurons per hidden layer. Each row of plots corresponds to different bit lengths ( $n_{bit}$ , ranging from 2 to 5). The results are averaged over ten independent trials.

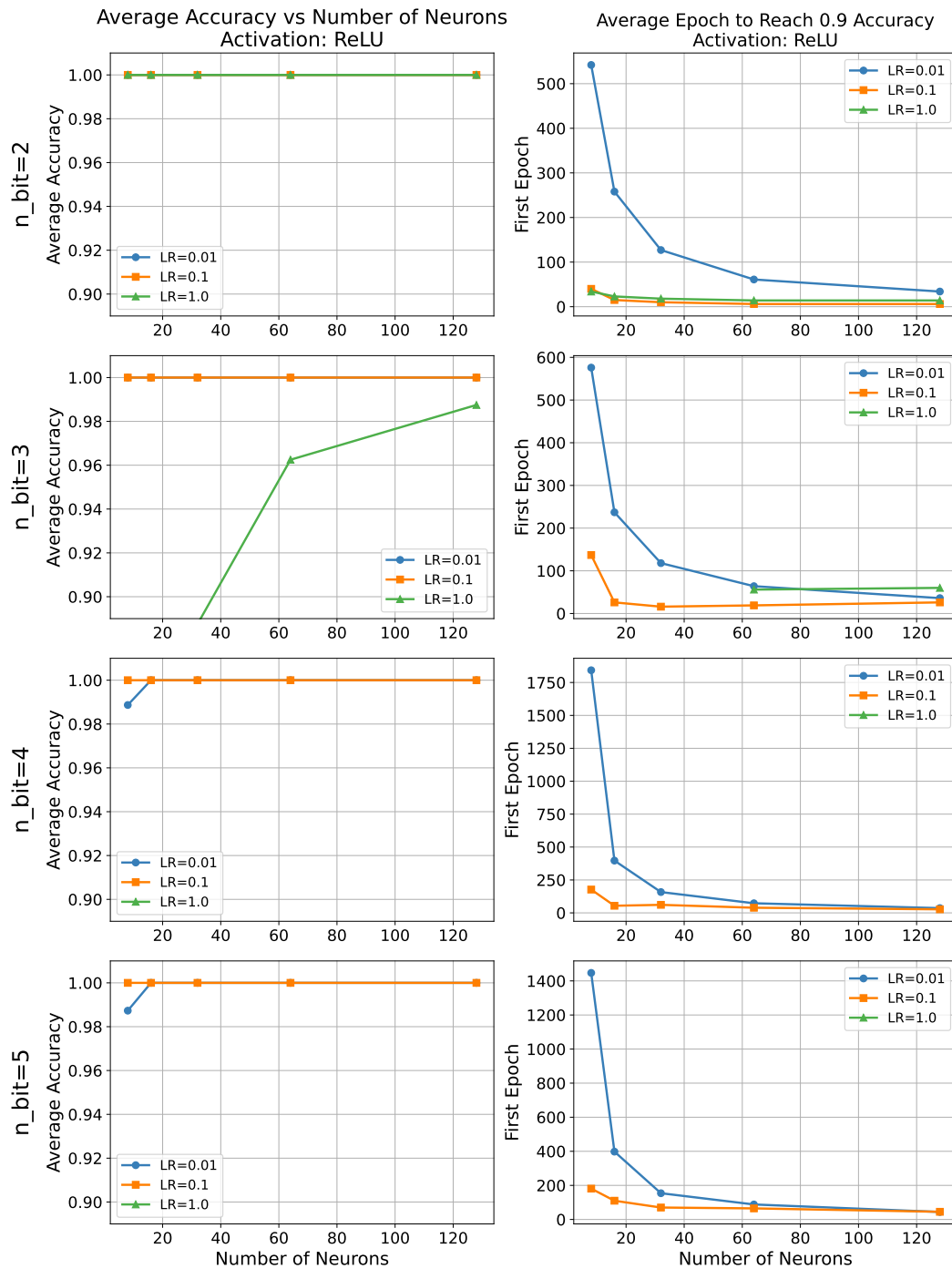


Figure 4: Performance of EDLA with ReLU activation function across various learning rates on the parity check task. The left column shows the accuracy of the EDLA network with the ReLU activation function as a function of neurons in a single hidden layer for different learning rates (LR = 0.01, 0.1, 1.0). The accuracies are average from 19900 to 20000 epochs. The right column shows the number of epochs required to achieve an accuracy of 0.9 against the number of neurons in the hidden layer for the same learning rates. Each row of plots corresponds to a different bit number ( $n\_bit$ ), ranging from 2 to 5, for the parity check task. The results are averaged over ten independent trials.

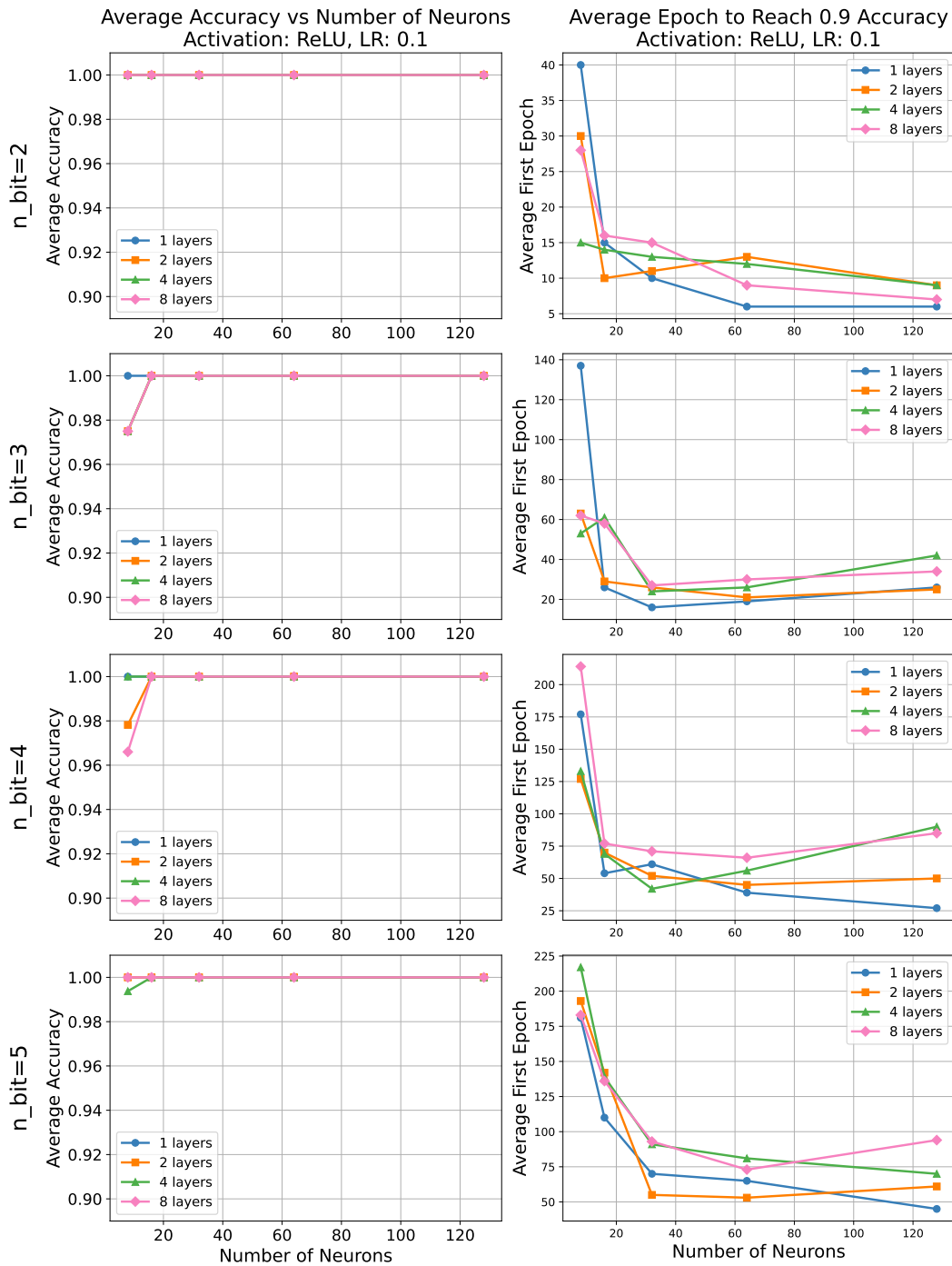


Figure 5: Accuracy and convergence characteristics of the EDLA network with ReLU activation function across various network depths (1, 2, 4, and 8 hidden layers), using a fixed learning rate of 1.0. The left column shows average classification accuracy as a function of neurons per hidden layer. The accuracies are average from 19900 to 20000 epochs. The right column presents the number of epochs required to reach an accuracy of 0.9 as a function of the number of neurons per hidden layer. Each row of plots corresponds to different bit lengths ( $n_{bit}$ ), ranging from 2 to 5. The results are averaged over ten independent trials.

samples with eight features and two target variables: heating and cooling loads. In this experiment, only the heating load is employed as the target variable, and the cooling load is not considered. The training and test datasets are randomly split into 80% and 20%, respectively, for all datasets.

The EDLA network consists of an input layer, hidden layers, and an output layer. The neurons in the input and the hidden layers use the sigmoid or ReLU activation functions. The neurons in the output layer use the linear activation function (i.e., no activation function). The training parameters are carefully selected for better performance, with a learning rate of 0.001 for sigmoid activation and 0.0001 for ReLU activation. Training is conducted for 500 epochs employing a mini-batch size of 64 samples.

Figure 6 illustrates the Mean Absolute Error (MAE) performance of the EDLA network across varying numbers of neurons (8, 16, 32, 64, 128, 256, 512, and 1024) and different layer configurations (1, 2, and 4 layers). The results indicate that EDLA networks with sigmoid activation function achieve efficient performance across all datasets, generally showing improvements as the number of neurons in the hidden layers increases. However, configurations employing 1024 neurons demonstrated performance degradation. Additionally, increasing the network depth beyond the two layers does not yield performance enhancements and exhibits deterioration compared with shallower network architectures. Furthermore, increased instability is observed in the behavior of the EDLA network as both the neuron count and the network depth increase. These observations collectively suggest that, while the EDLA approach is adequately capable for regression tasks, augmenting the number of neurons and network depth does not necessarily improve performance.

### 5.3 Image Classification Tasks

To evaluate the performance of the EDLA network in image classification tasks, the experiments are conducted using the handwritten digits dataset (Digits), MNIST, and Fashion MNIST datasets. The Digits used consists of 5620 grayscale images with a resolution of  $8 \times 8$  pixels. The Digits is not divided into training and test datasets. In this study, 20 % of the entire dataset is randomly selected and used as test data. The MNIST comprises 60,000 training and 10,000 testing grayscale images of handwritten digits, each with a resolution of  $28 \times 28$  pixels. Similarly, the Fashion-MNIST includes 60,000 training and 10,000 testing grayscale images of fashion articles at a resolution of  $28 \times 28$  pixels.

The EDLA network consists of an input layer, a hidden layer, and an output layer. The neurons in the input and hidden layers utilize sigmoid or ReLU activation functions. The output layer employs the sigmoid activation function. To assess its performance across various configurations, the number of neurons in each hidden layer is varied systematically. The learning rates when using the sigmoid and ReLU activation functions are 1.0 and 0.1, respectively. The network is trained for 500 epochs. We employed the minibatch method and set the minibatch size to 128 samples.

Figure 7 illustrates the performance of the EDLA network using the sigmoid activation function for various numbers of neurons in each hidden layer. Across all datasets, the classification performance generally improved as the number of neurons in the hidden layers increased. Specifically, for the Digits dataset, near-perfect accuracy is rapidly achieved, even with a relatively small number of neurons. For the MNIST and Fashion MNIST datasets, while high accuracy is attained, a larger number of neurons contributed to an incrementally improved performance. However, the depth of the EDLA network does not improve the performance, but worsens the performance. In terms of the reach epoch, for all configurations, the EDLA network shows a sufficiently fast reach of 0.8 accuracy. While deeper networks will lead to a slower reach, the number of neurons in each hidden layer will lead to a faster reach.

Similarly, Figure 8 shows the performance of the EDLA network using the ReLU activation function across varying numbers of neurons in each hidden layer. The results reveal that the EDLA network with ReLU achieves a performance comparable to that of a sigmoid-based network. However, for ReLU activation, deeper networks lead to worse performance. Furthermore, for a deeper network, the number of neurons in each hidden layer leads to worse performance. The reach epoch for ReLU activation decreases with the number of neurons in each hidden layer. However, the reach epoch for deeper networks will lead to a slower reach.

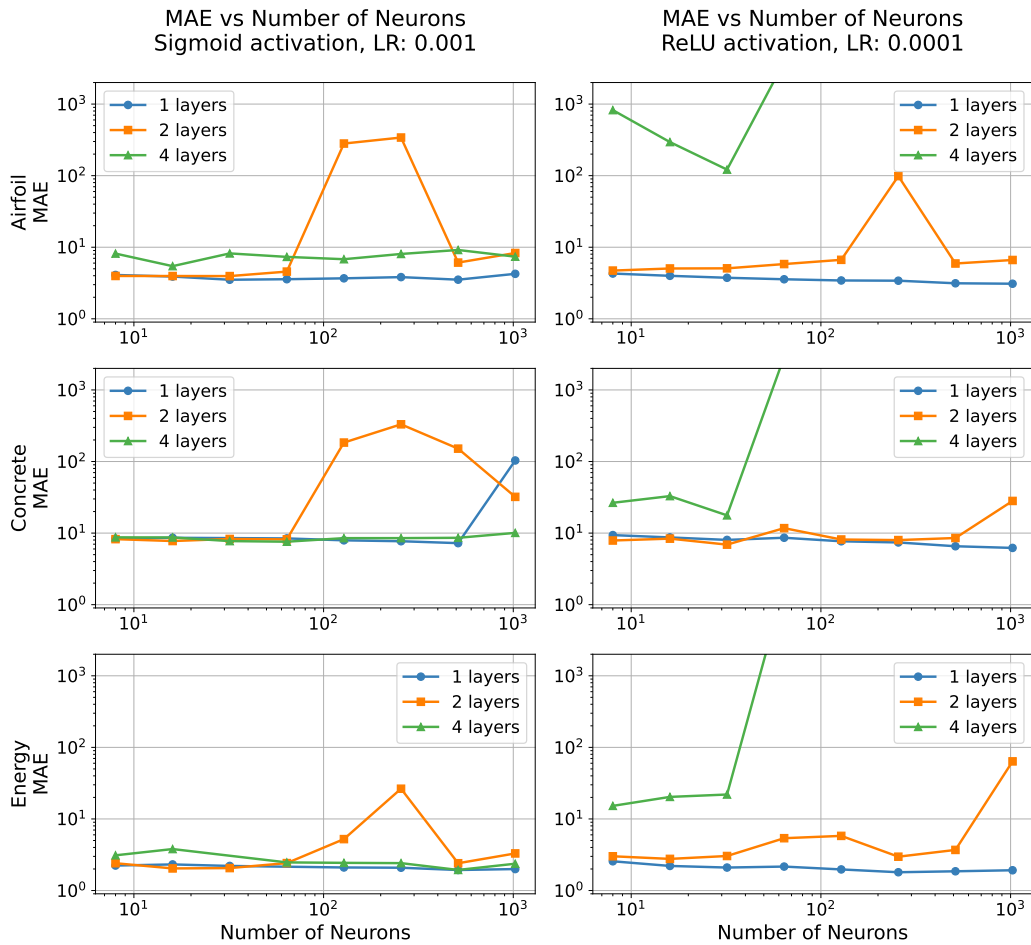


Figure 6: Performance of the EDLA network on regression datasets across varying layer configurations. The left column shows the Mean Absolute Error (MAE) for sigmoid activation, while the right column displays the MAE for ReLU activation. Both sets of results are plotted as a function of the number of neurons per hidden layer for 1, 2, and 4 hidden layers. Each row corresponds to the Airfoil Self-Noise dataset (top row), Concrete Compressive Strength dataset (middle row), and Energy Efficiency dataset (bottom row). Missing data points in the figure signify that the network output became excessively large or yielded a not-a-number (NaN) value. The results are averaged over four independent trials.

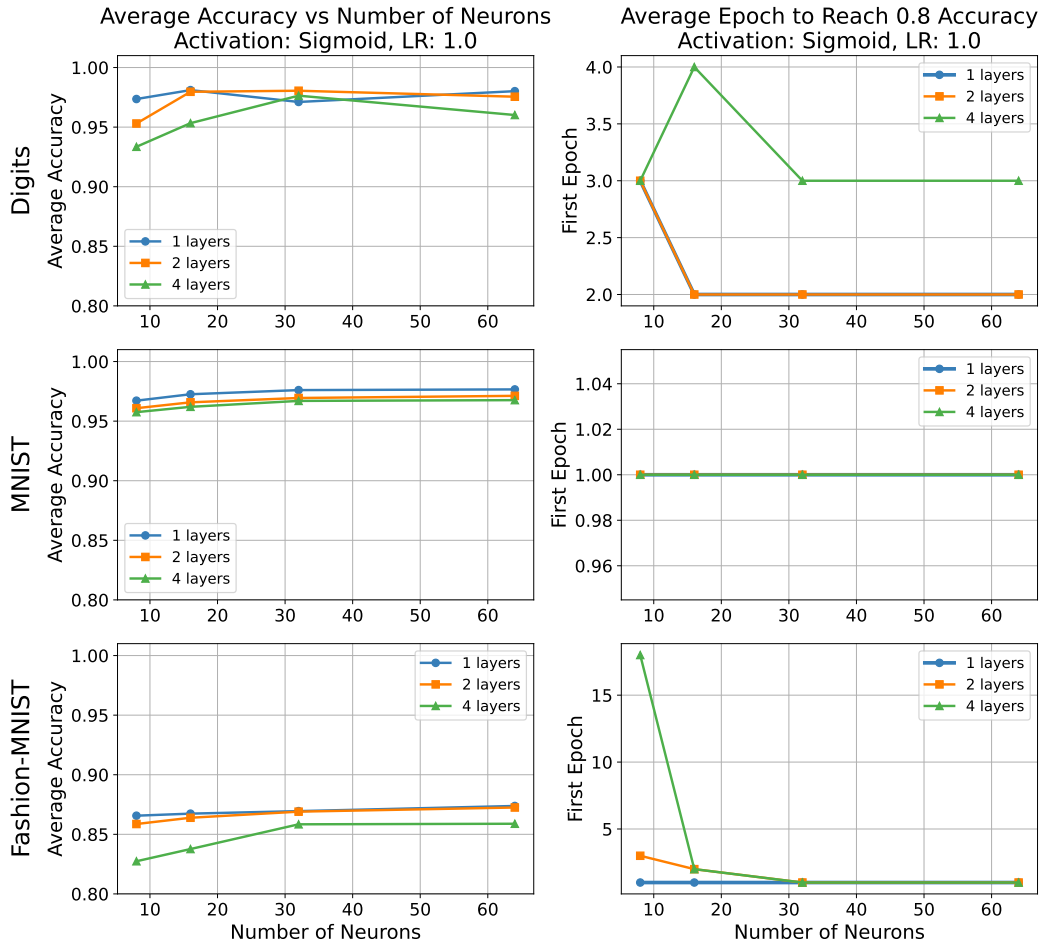


Figure 7: Performance of EDLA with sigmoid activation on image datasets across layer configurations. The plots in the left column show the accuracy of the EDLA network with the sigmoid activation as a function of the number of neurons in each hidden layer for different layer configurations (1, 2, and 4 layers) across three datasets: digits, MNIST, and fashion\_MNIST. The plots in the right column illustrate the number of epochs required to achieve an accuracy of 0.8 against the number of neurons in each hidden layer for the same layer configurations. The results are averaged over four independent trials.

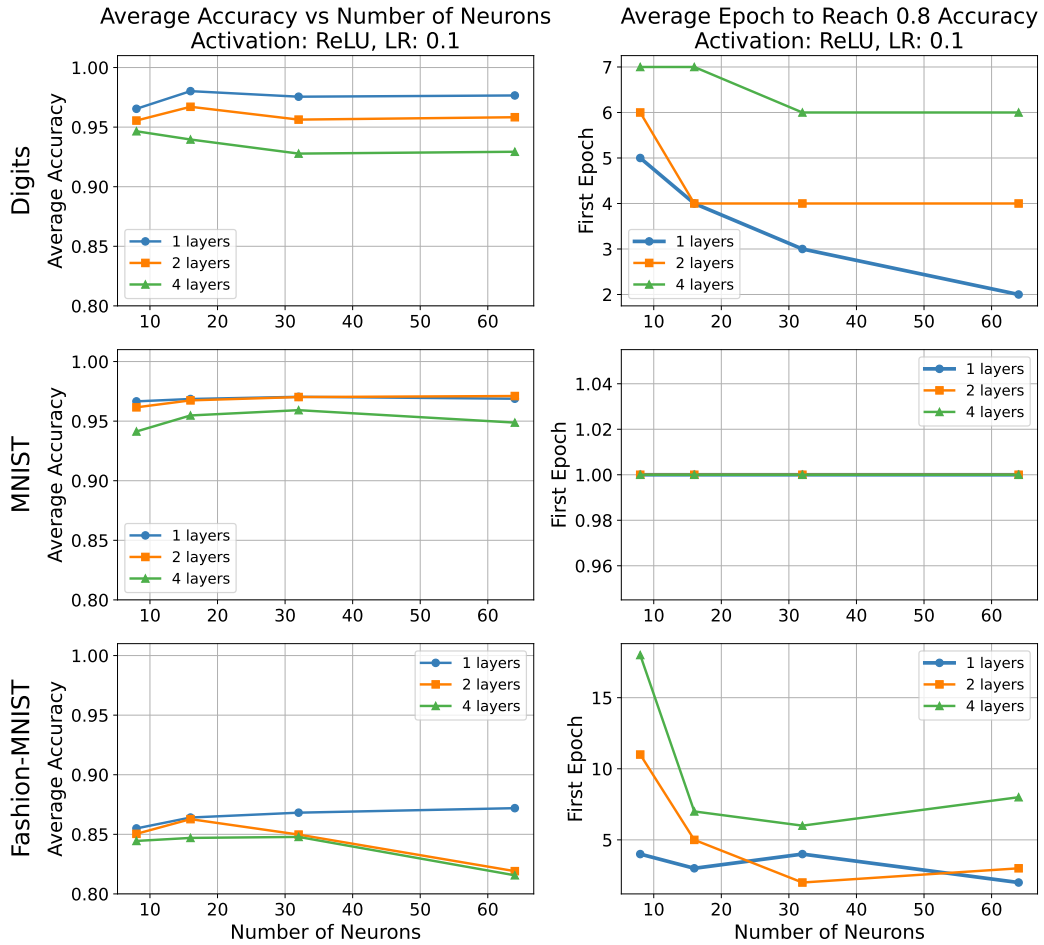


Figure 8: Performance of EDLA with ReLU activation on image datasets across layer configurations. The plots in the left column show the accuracy of the EDLA network with the sigmoid activation as a function of the number of neurons in each hidden layer for different layer configurations (1, 2, and 4 layers) across three datasets: digits, MNIST, and fashion\_MNIST. The plots in the right column illustrate the number of epochs required to achieve an accuracy of 0.8 against the number of neurons in each hidden layer for the same layer configurations. The results are averaged over four independent trials.

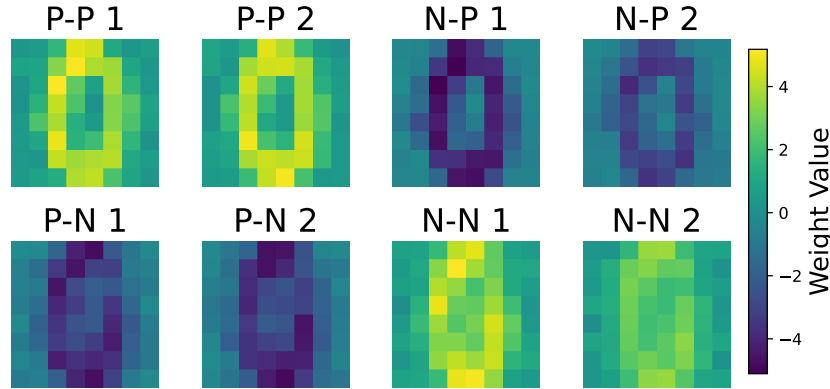


Figure 9: A heatmap of the synaptic weights connecting the input layer to the first hidden layer in the EDLA network is trained to classify the digit “zero” in the Digits dataset. Each subplot shows the weight patterns for individual connection patterns, labeled according to connection types: P-P (positive input to positive hidden sublayers), N-P (negative input to positive hidden sublayers), P-N (positive input to negative hidden sublayers), and N-N (negative input to negative hidden sublayers). Color gradients denote weight values, with yellow indicating strongly positive weights and purple indicating strongly negative weights. Histogram of synaptic weight distribution in the EDLA Network. The horizontal axis denotes the synaptic weight values, and the vertical axis indicates the corresponding frequencies.

#### 5.4 Analysis of Internal Representations

In this section, we investigate the internal representations learned by the EDLA network by analyzing the synaptic weights in the hidden layers. The experiments use an EDLA network with a single hidden layer containing two neurons with sigmoid activation functions. The network is trained on the Digits dataset for over 500 epochs.

Figure 9 shows a heatmap of the synaptic weights connecting the input layer to the hidden layer within the EDLA network, specifically trained to classify the digit “zero” from handwritten digits. The heatmap reveals that the network learned meaningful features from the input data. Notably, the neurons in the hidden layer exhibit a strong response to specific patterns within the images. For instance, the weights connecting the positive neurons in the input layer to the positive neurons in the hidden layer (denoted as "P-P" connections) show high activation, shaping the digit “zero.” This result suggests that the EDLA method effectively enables neurons to capture and represent the relevant digit-specific features. Additionally, similar "zero-shaped" patterns also emerge in other synaptic connections.

Synaptic weight distributions in neural networks provide valuable insights into the learning behavior of the network and features extracted from the input data. To explore this further, we analyze the distribution of weights across the EDLA network. Figure 10 shows a histogram representing the synaptic weights within the trained EDLA network. The distribution appears to be predominantly centered around small magnitudes, indicating that most weights are relatively small. However, a distinct spread is observed with a smaller subset of synapses exhibiting large positive or negative values. This broad distribution suggests that the EDLA update unilaterally increased the absolute values of the weights while balancing the excitatory and inhibitory weights.

## 6 Conclusion

The Error Diffusion Learning Algorithm (EDLA) provides a biologically inspired alternative to conventional backpropagation methods for training neural networks and is characterized by the diffusion of a global error signal across network layers. This mechanism is analogous to reward-based learning processes observed in biological neural systems. Specifically, a positive reward prediction error (RPE) strengthens synapses by increasing the likelihood of repeating rewarded actions, whereas a negative RPE weakens them. Moreover, the EDLA mirrors neuromodulatory systems, such as the

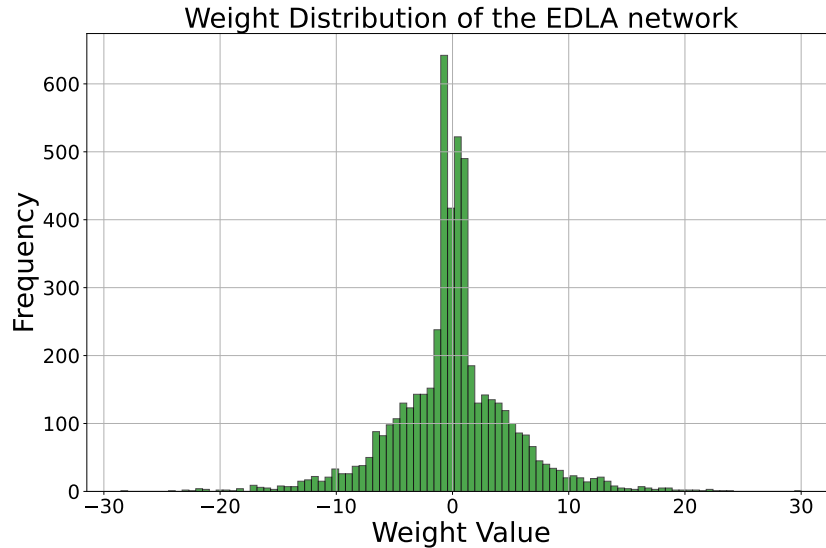


Figure 10: Histogram of synaptic weight distribution in the EDLA Network. The horizontal axis denotes the synaptic weight values, and the vertical axis indicates the corresponding frequencies.

dopaminergic system, which projects broadly across cortical and subcortical areas, disseminating their signals globally Roelfsema and Holtmaat (2018). In contrast to standard MLPs, the EDLA incorporates structured interactions between neurons with excitatory and inhibitory synapses. This reflects the biologically observed balance between these types of synapses.

However, EDLA is inherently restricted by its single-output architecture, which limits its applicability in multiclass classification tasks. A practical solution involves parallelizing multiple EDLA networks, although this approach increases computational costs. This parallelized architecture mirrors the modular structure of biological neural systems in which specialized circuits process distinct features or tasks independently. In such a configuration, each EDLA network separately optimizes its own output according to a unique global error signal to that network. This modular structure aligns with distributed processing mechanisms observed in biological neural networks.

The EDLA demonstrates efficacy across various tasks, including parity checks, regression, and image classification. Experimental evaluations indicate that the EDLA achieves a satisfactory performance across various datasets. Notably, the ReLU activation function achieves a performance comparable to that of the sigmoid function originally proposed by Kaneko Kaneko (2008), where the ReLU often converges more quickly. However, because the ReLU lacks an upper bound, it can produce huge and potentially unstable weight updates under the Hebbian-like learning dynamics employed by the EDLA. Moreover, while increasing the number of neurons in a hidden layer will improve performance and accelerate convergence, excessive network depth or an overly large number of hidden neurons may degrade performance because of unstable weight updates. A reduction in the learning rate can mitigate these instabilities.

In contrast to backpropagation, which requires error signals to be propagated backward through each intermediate layer, EDLA relies solely on a single global error signal combined with local neural activities. This approach presents potential advantages for developing more biologically plausible neural network training techniques. Thus, the EDLA will represent a significant step toward bridging the gap between biological realism and artificial neural network methodologies.

## References

- E. D. Adrian. The all-or-none principle in nerve. *The Journal of Physiology*, 47(6):460–474, 1914.
- Manuel Casanova and Emily Casanova. The modular organization of the cerebral cortex: Evolutionary significance and possible links to neurodevelopmental conditions. *Journal of Comparative Neurology*, 527, 10 2018. doi: 10.1002/cne.24554.

- Donald O. Hebb. *The organization of behavior: A neuropsychological theory*. Wiley, New York, 1949.
- D. H. Hubel and T. N. Wiesel. Receptive fields and functional architecture of monkey striate cortex. *The Journal of Physiology*, 195(1):215–243, 1968. doi: <https://doi.org/10.1113/jphysiol.1968.sp008455>. URL <https://physoc.onlinelibrary.wiley.com/doi/abs/10.1113/jphysiol.1968.sp008455>.
- Isamu Kaneko. Sample programs of error diffusion learning algorithm. <https://web.archive.org/web/20000306212433/http://village.infoweb.ne.jp/~fwhz9346/ed.htm>, 2008. [Online; accessed 20-Sep-2024].
- Genichi Kato. The general idea of the theory of decrementless conduction. *Proc. Imp. Acad.*, 2(5): 233–235, 1926.
- S.C. Kleene. Representation of events in nerve nets and finite automata. *Annals of Mathematics Studies*, 34:3–41, 1956.
- Yann LeCun, Yoshua Bengio, and Geoffrey Hinton. Deep learning. *nature*, 521(7553):436, 2015.
- Hong Li and Michael C. Crair. How do barrels form in somatosensory cortex? *Annals of the New York Academy of Sciences*, 1225(1):119–129, 2011. doi: <https://doi.org/10.1111/j.1749-6632.2011.06024.x>. URL <https://nyaspubs.onlinelibrary.wiley.com/doi/abs/10.1111/j.1749-6632.2011.06024.x>.
- Warren McCulloch and Walter Pitts. A logical calculus of ideas immanent in nervous activity. *Bulletin of Mathematical Biophysics*, 5:127–147, 1943.
- Vernon B. Mountcastle. Modality and topographic properties of single neurons of cat's somatic sensory cortex. *Journal of Neurophysiology*, 20(4):408–434, 1957. doi: 10.1152/jn.1957.20.4.408.
- Pieter Roelfsema and Anthony Holtmaat. Control of synaptic plasticity in deep cortical networks. *Nature Reviews Neuroscience*, 19:166–180, 02 2018. doi: 10.1038/nrn.2018.6.
- Frank Rosenblatt. The perceptron: A probabilistic model for information storage and organization in the brain. *Psychological Review*, 65(6):386–408, 1958. doi: 10.1037/h0042519.
- David E Rumelhart, Geoffrey E Hinton, and Ronald J Williams. Learning representations by back-propagating errors. *nature*, 323(6088):533–536, 1986.
- Takayuki Sato, Go Uchida, and Manabu Tanifuji. Cortical columnar organization is reconsidered in inferior temporal cortex. *Cerebral Cortex*, 19(8):1870–1888, 12 2008. ISSN 1047-3211. doi: 10.1093/cercor/bhn218. URL <https://doi.org/10.1093/cercor/bhn218>.
- Keiji Tanaka. Inferotemporal cortex and object vision. *Annual Review of Neuroscience*, 19:109–139, 1996. doi: 10.1146/annurev.ne.19.030196.000545.
- Thomas A. Woolsey and Hendrik Van der Loos. The structural organization of layer iv in the somatosensory region (s i) of mouse cerebral cortex: The description of a cortical field composed of discrete cytoarchitectonic units. *Brain Research*, 17(2):205–242, 1970. ISSN 0006-8993. doi: [https://doi.org/10.1016/0006-8993\(70\)90079-X](https://doi.org/10.1016/0006-8993(70)90079-X). URL <https://www.sciencedirect.com/science/article/pii/000689937090079X>.